Hull Girder Fatigue Damage Estimations of a Large Container Vessel by Spectral Analysis

Andersen, Ingrid Marie Vincent; Jensen, Jørgen Juncher

Published in:
Proceedings of the PRADS 2013

Publication date:
2013

Proceedings of the PRADS2013
20-25 October, 2013
CECO, Changwon City, Korea

Hull Girder Fatigue Damage Estimations of a Large Container Vessel by Spectral Analysis

Ingrid Marie Vincent Andersen and Jørgen Juncher Jensen

Technical University of Denmark

Abstract

This paper deals with fatigue damage estimation from the analysis of full-scale stress measurements in the hull of a large container vessel (9,400 TEU) covering several months of operation.

For onboard decision support and hull monitoring systems, there is a need for a fast reliable method for estimation of fatigue damage in the ship hull.

The objective of the study is to investigate whether the higher frequency contributions from the hydroelastic responses (springing and whipping) can satisfactory be included in the fatigue damage estimation by only a few parameters derived from the stress power spectrum as an alternative to rainflow counting.

The outcome of rainflow counting is compared with the results of a narrow-band spectral analysis as well as the outcome of three approaches considering the process as bimodal in order to take the hydroelastic responses into account.

In most cases, the spectral analysis show satisfactory agreement with the results from rainflow counting.

Keywords

Fatigue damage estimation; container ship; rainflow counting; spectral methods; bimodal processes; Gaussian processes; decision support.

Introduction

The EU project TULCS (Tools for Ultra Large Container Ships) is concerned with the influence of hydroelastic structural responses, such as springing and whipping, of large container ships and their implications on design. For ocean going ships, fatigue is the governing failure mode and the hydroelastic responses may contribute significantly to additional hull girder loads which should be taken into consideration in the design and operation of ultra large ships.

A ship sailing in a seaway is subject to wave induced random excitations of the hull at mainly the wave encounter frequency and at the vertical bending natural frequency of the hull. As such, the response cannot be considered narrow-banded but, however, the narrow-band approximation is sometimes used as a conservative estimate of the fatigue damage. For onboard monitoring of the accumulated fatigue damage, a fast, reliable method is needed for the estimation.

Time domain analysis of long time series is accurate but computationally expensive and one may instead choose to analyse the power spectral density, which is computationally simpler, only requires a few parameters derived from the power spectrum of the stress response and can be done using the various approaches described in the present paper. Spectral methods generally yield conservative results and attempts have been made to reduce the conservatism of the spectra methods using a bimodal approach.

Data Collection

The data was collected during the TULCS project on board a 9,400 TEU container vessel built in 2006. The main dimensions of the ship are given in Table 1.

Table 1: Main dimensions of ship.

L_{OA}	349.0 m
Beam	42.8 m
Draught	15.0 m
DWT	113,000 ton

The fatigue damage analysis is carried out for three days of operation: 12 August 2011 (Gulf of Aden, going West, moderate sea state), 20 September 2011 (South of India, going East mild sea state) and 2 October 2011 (off Hong Kong, going North West, severe sea state). For each day, 24 hours of data is available. Information about the sea state (significant wave height, peak period and relative wave direction) is obtained from a WaMoS II ® wave radar system installed on the bridge of the vessel as part of the data collection for the TULCS project. The WaMoS data for the relevant voyage parts is illustrated in Appendix A, Fig. A1-A3. The WaMoS parameters are recorded every 5 min.

The approximate encountered range of significant wave height H_S is summarized in Table 2.

Table 2: Range of H_S for the three analysed days from the onboard WaMoS system.

Date	H_S
12 Aug 2011	1-5 m
20 Sep 2011	1.3-1.7 m
02 Oct 2011	3-10 m

It is noted that the considered WaMoS system is generally thought to overestimate H_S for higher sea states. Furthermore, it is noted that the conditions on 12 August 2011 are starting out calm with the sea state building up during the 24 hours while the opposite is the case for 02 October. Please also refer to Nielsen and Andersen (2013), where a detailed comparison between the WaMoS data and wave estimations based on analysis of the ship motions is given.

Two long base strain gauges of the displacement measuring type are installed amidships in port and starboard side respectively as illustrated in Fig. 1 and Fig. 2.

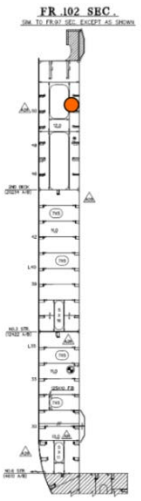

Fig. 1: Location of long base strain gauge close to the deck amidships. From MARIN (2007).

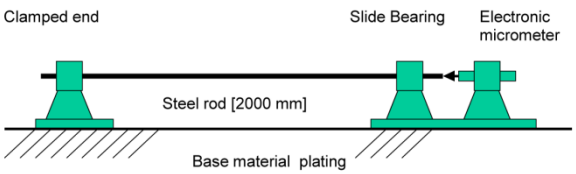

Fig. 2: Working principle of the long-base strain gauge. From MARIN (2007).

The strain measurements are sampled at 20 Hz and converted into stress signals.

The mean of the port and starboard signal is taken and used to exclude the possible contributions from horizontal and torsional stress components. Elongation is measured as positive and thus a hogging condition yields positive strain values while the sagging condition yields negative values.

In order to distinguish between the wave frequency (WF) and the high frequency (HF) contribution to the fatigue damage the dividing frequency must be determined. This is done most conveniently from examining the response power spectrum, i.e. the Fast Fourier Transform (FFT) of the stress time history illustrated in Fig. 3 and Fig. 4 for two different sea states. The dividing frequency between the wave frequency part and the high frequency part is set to 2 rad/s (0.32 Hz) as illustrated by the change of colour and as recommended by American Bureau of Shipping (2010). Note that the axes on the two plots are not the same. For the data from 12 August in Fig. 3 there are two contributing main encounter wave frequencies and the process is clearly broad-banded.

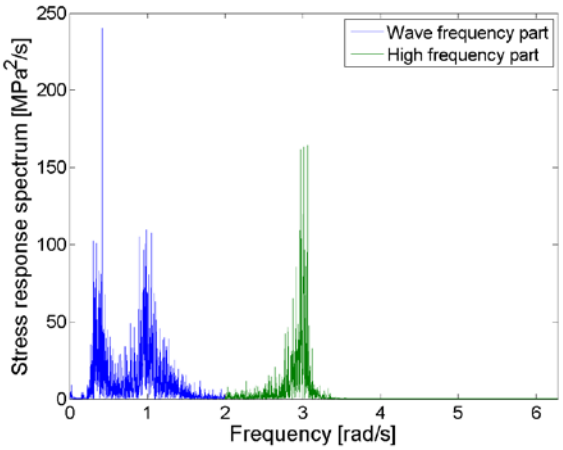

Fig. 3: FFT of stress time series with wave frequency response and high frequency response outlined. The 2nd node natural vertical vibration frequency of the hull is seen at about 3 rad/s. FFT of one hour of data from 12 August 2011 @ 8 hours.

For the data from 02 October in Fig. 4 the process is clearly bimodal and much closer to being narrow-banded and the two spectra are well-separated.

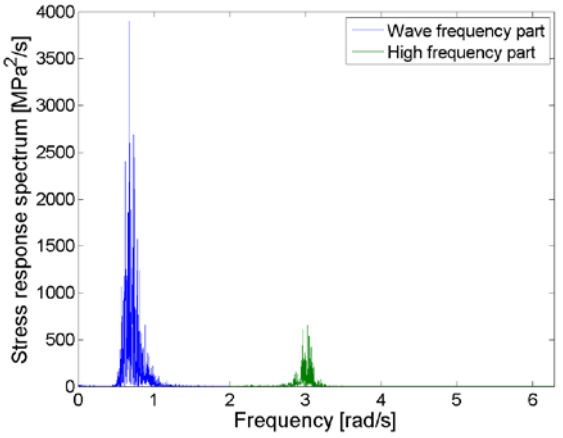

Fig. 4: FFT of stress time series with wave frequency response and high frequency response outlined. The 2nd node natural vertical vibration frequency of the hull is seen at about 3 rad/s. FFT of one hour of data from 02 October 2011 @ 10 hours.

In the high frequency tail the signal is cut off at 1.6 Hz (10 rad/s) to reduce noise and in the low frequency end contributions with a period over 50 seconds are filtered out. The filter-

ing of the wave and high frequency components is carried in the frequency domain using FFT and inverse FFT. An example of a time series before and after filtering is given in Fig. 5.

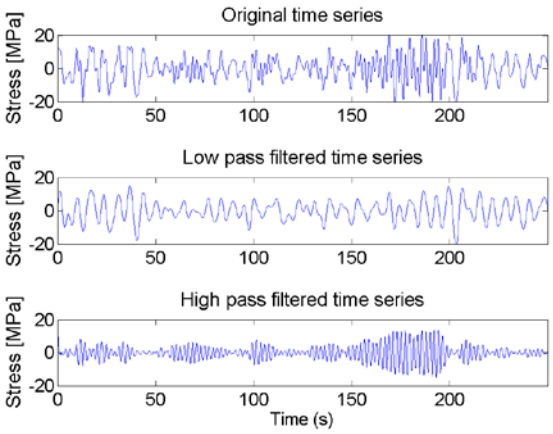

Fig. 5: Original, low pass and high pass filtered time series signal of stress (average of port and starboard side). Data from 12 Aug 2011 @ 00 hours.

Fatigue Damage Estimation

Fatigue life of structures can basically be estimated using two different approaches. Assuming stochastic vibrational loads and no sequence effects, the fatigue damage can be estimated in the time domain using a cycle count method, such as rainflow counting (RFC) where the stress cycles which contribute to fatigue are counted and a fatigue model such as the linear Palmgren-Miner rule is subsequently applied. RFC in combination with application of the Palmgren-Miner rule is the most commonly used approach when assessing fatigue life of structures.

Spectral methods for fatigue damage estimation are computationally faster and can therefore be preferred in some cases – particularly for application in onboard decision support systems.

Traditionally, for the spectral analysis it is simply assumed that the entire load history is narrow-banded and Gaussian. However, when hydroelastic effects play a role, the vibrational response of the hull girder of a container ship is usually more broad-banded and thus the narrow-band formulation yields conservative damage estimation.

Instead of assuming that the total process is narrow-banded it can be argued, that the two individual frequency components of the response considered here can be taken as narrow-banded and an assumption of bi-modal response spectra can be used to reduce the conservativeness of the narrow-band assumption cf. e.g. Jiao & Moan (1990) and Low (2010). In the present paper more than one elastic global vibrational mode is not considered relevant for fatigue damage analysis in the hull girder.

In the following analysis one hour of data is treated at the time, which is considered enough to make the RFC results stable. For the individual illustration of the methods only the results from 12 August (moderate sea state) are plotted due to space constrains. However, for the comparison of the five treated methods the total estimate fatigue damage is illustrated for all three of the analysed days.

Rainflow Counting and the Palmgren-Miner Rule

The rainflow counting is carried out on the wave frequency part of the stress signal and on the total signal. Cf. Storhaug & Moe (2007), the WF and HF contributions should not be considered two independent signals and thus the HF damage should not be assessed using a direct rainflow count of the high frequency part of the signal. Thus, the high frequency contribution to the damage is taken as the difference between the total fatigue damage and the wave frequency damage.

A log-scale factor SN-curve with the slope $m = 3$ and $\log(K) = 12.65$ is used in all cases. No stress concentration factor is included.

The results of the RFC for 12 August 2011 are found in Fig. 6. For the three analysed time periods the hydroelastic effects are more or less pronounced. For 12 August and 02 October (not shown) the high frequency part is observed to contribute with a very significant part (more than half) of the total estimated fatigue damage, while the high frequency effect for 20 September (not shown), where the sea state was mild, is negligible.

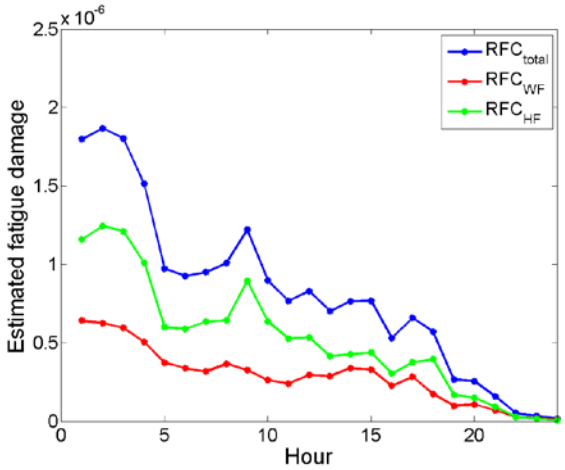

Fig. 6: Fatigue damage per hour during 24 hours on 12 August 2011 estimated using rainflow counting and the Palmgren-Miner rule.

One Narrow-banded Gaussian Process

Assuming that the total load history is a stationary, narrow-banded and Gaussian process, the expected damage D_{NB} over the time T is, cf. e.g. Jiao & Moan, (1990) given by the Raleigh approximation to the fatigue damage:

$$\bar{D}_{NB} = \frac{\nu_0 T}{K}\left(2\sqrt{2}s\right)^m \Gamma\left(\frac{m}{2}+1\right) \quad (1)$$

where ν_0 is the zero-upcrossing rate of the total process, s is the standard deviation, and Γ is the gamma function. Like for the RFC analysis, the narrow-band analysis is carried out for the total and the WF part of the signal and the HF part is taken as the difference between the total and the WF part. The outcome of the narrow-banded spectral analysis for 12 August is illustrated in Fig. 7. The estimated fatigue damage is quite similar to that of the RFC analysis but, as expected, generally higher and the narrow-band formulation generally attributes slightly more influence to the HF part compared to RFC.

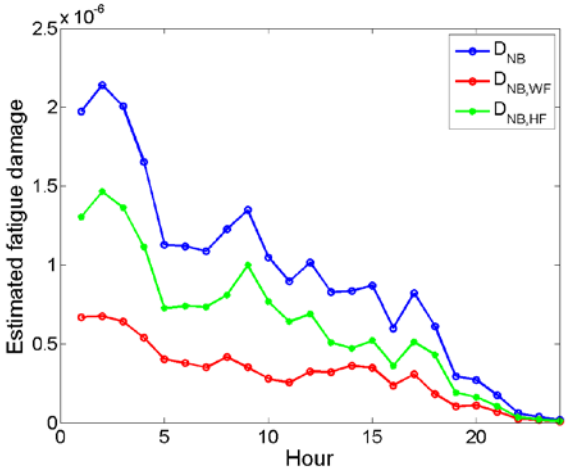

Fig. 7: Fatigue damage during 24 hours on 12 August 2011 estimated using narrow-banded spectral analysis.

Combination of a Stationary Gaussian Process and a Non-Gaussian Transient Process

In the approach suggested by Jiao & Moan (1990), the process can be assumed composed by a narrow-banded Gaussian process and a transient component, which is typically the case for slamming induced loads in ships. Results from Nielsen et. al. (2011) indicate that it may be an accurate approximation to combine a stationary Gaussian process at wave frequency and with a transient response assuming Rayleigh distributed transient peaks. In this analysis, the stationary part corresponds to the low pass filtered wave frequency signal and the transient part to the high pass filtered signal, cf. Fig. 3, Fig. 4 and Fig. 5. The total damage can be estimated as the sum of the damage from the envelope process, D_E and the transient process D_2. The inter-arrival time between each transient event T_0 is to be included in Eq. (1) in the estimation of the damage from the envelope process:

$$\overline{D}_E = \frac{\nu_{0,WF} T}{K} \left(2\sqrt{2} s_{WF}\right)^m \Gamma\left(\frac{m}{2}+1\right) \eta T_0 \qquad (2)$$

The estimated fatigue damage caused by the transient process during the time period T, can be expressed by

$$\overline{D}_2 = \frac{T}{T_0 K} \left(2\sqrt{2} s_{HF}\right)^m \Gamma\left(\frac{m}{2}+1\right) \frac{1}{1-e^{-2\pi\xi m}} \qquad (3)$$

where ξ is the total structural damping ratio; here taken as 1% in all cases in accordance with findings in Storhaug and Moe (2007). The term ηT_0 in Eq. (2) is expressed by Jiao & Moan (1990) as:

$$\eta T_0 = \frac{1}{T_0}\int_0^{T_0} \frac{1-\theta e^{-\xi\omega_{HF}t}}{[1+\theta^2 e^{-2\xi\omega_{HF}t}]^3}\mathrm{d}t + \frac{\sqrt{\pi}\theta m \Gamma\left(\frac{m}{2}+\frac{1}{2}\right)}{T_0 \Gamma\left(\frac{m}{2}+1\right)} \times \int_0^{T_0} e^{-\xi\omega_{HF}t}\left[1+\theta^2 e^{-2\xi\omega_{HF}t}\right]^{\frac{m}{2}-2}\mathrm{d}t \qquad (4)$$

where $\omega_{HF} = 2\pi\nu_{0,HF}$. Setting m = 3 the integrals in Eq. (4) can be evaluated analytically by substituting $u = \theta e^{-\xi\omega_{HF}t}$ as shown by Nielsen et. al. (2011).

The total estimated fatigue damage during the time T is thus the sum of D_E and D_2 as illustrated in Fig. 8 for 12 August 2011.

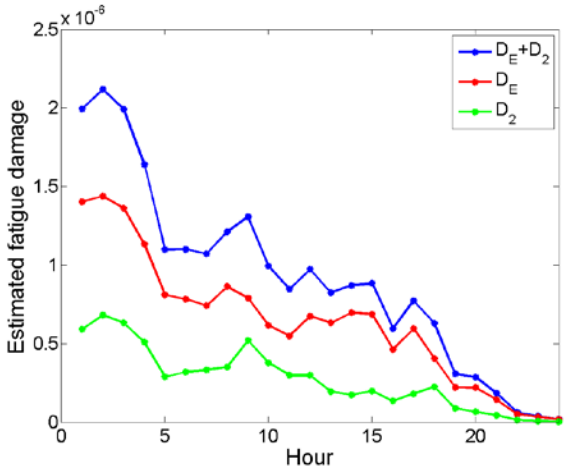

Fig. 8: Fatigue damage during 24 hours on 12 August 2011 estimated using a combination of a Gaussian and a transient process. T_0 = 10 sec.

The damage due to the small cycles, D_2, is found the play a considerable role for two of the days (12 August and 02 October) and it can be concluded from the observed data that the contribution from the transient process D_2 cannot generally be neglected contrarily to findings in Nielsen et. al. (2011).

According to Jiao & Moan (1990) the Gaussian and the transient part are assumed being statistically independent, which is not generally the case for a ship, since the transient vibration is usually initiated by a slam which occurs together with a large sagging response. Here, T_0 = 10 sec matches the RFC results best. 10 sec may appear as a very short inter-arrival time between the transient events. However, the use of a relatively small T_0 is justified by findings in Nielsen et. al. (2011) and by additional analysis carried out in connection with the preparation of the present paper.

This method has a disadvantage in being rather sensitive to the manual choice of inter-arrival time.

Combination of two Narrow-banded Gaussian Processes using the Envelope Process

Using another approach, also suggested by Jiao & Moan (1990), the broad-banded process can be considered consisting of two individual, statistically independent narrow-banded stationary Gaussian processes at low and high frequency, which is common in engineering problems such as ships encountering loads at the exciting wave frequency and vibrational loads excited at the lowest natural frequency of the hull. In the bimodal approach, the total process can be assumed modelled by a wave frequency and a high frequency component:

$$X(t) = X_{WF}(t) + X_{HF}(t)$$

The spectra of the two components are assumed non-overlapping and thus the processes are statistically independent. The total expected damage is thus the sum of the contributions from the wave frequency and high frequency components (large and small cycles, respectively for this method):

$$\bar{D} = \bar{D}_L + \bar{D}_S$$

For the large cycles the damage is estimated from the envelope of the total process (Jiao & Moan, 1990, Eq. (39)):

$$\bar{D}_L = \frac{2^m \nu_{0,E} T}{K} \int_0^\infty r^m f_{R_L}(r) \mathrm{d}r \tag{5}$$

where $f_{R_L}(r)$ is the amplitude distribution of the large-cycle envelope stress amplitude R_L. In order to avoid numerical integration of Eq. (5) Low (2010) suggested dividing R_L into the WF and HF parts:

$$R_L = R_{WF} + R_{HF} \tag{6}$$

As these two terms can be assumed statistically independent Eq. (5) can be re-written as:

$$D_L = \frac{2^m \nu_{0,E} T}{K} \int_0^\infty f_{R_{WF}}(r_{WF}) \int_0^\infty [r_{HF} + r_{WF}]^m \times f_{R_{HF}}(r_{HF}) \mathrm{d}r_{HF} \mathrm{d}r_{WF} \tag{7}$$

where $\nu_{0,E}$ is the zero upcrossing rate of the envelope process:

$$\nu_{0,E} = \nu_{0,WF} \frac{\sqrt{1 + (\theta\beta\delta_{HF})^2}}{1 + \theta^2} \tag{8}$$

Furthermore, in Eq. (8), θ describes the relative dominance of the high frequency contribution, β describes the spacing between the low and high frequency parts and, δ_{HF} is the bandwidth parameter of the high frequency process:

$$\theta = \frac{s_{HF}}{s_{WF}} \tag{9}$$

$$\beta = \frac{\nu_{0,HF}}{\nu_{0,WF}} \tag{10}$$

$$\delta_{HF} = \sqrt{1 - \frac{\lambda_{1,HF}^2}{\lambda_{0,HF}\lambda_{2,HF}}} \tag{11}$$

In Eq. (11) λ_i denotes the *i*'th spectral moment of the process. By writing the integral in Eq. (5) as double integration as done in Eq. (7) the exact result can be found in terms of a binomial series with $m + 1$ terms as suggested by Low (2010):

$$\bar{D}_L = \frac{\left(2\sqrt{2}\right)^m \nu_{0,E} T}{K} \sum_{k=0}^{m} \binom{m}{k} s_{HF}^k \times s_{WF}^{m-k} \Gamma\left(1 + \frac{k}{2}\right) \Gamma\left(1 + \frac{m-k}{2}\right) \tag{12}$$

The damage from the small cycles, D_S, is calculated from the narrow-band high frequency process in accordance with Eq. (1):

$$\bar{D}_S = \frac{\nu_{0,HF} T}{K} \left(2\sqrt{2} s_{HF}\right)^m \Gamma\left(\frac{m}{2} + 1\right)$$

The outcome of the approach described above is illustrated in Fig. 9 for 12 August 2011. Note, that the large and small cycle contributions cannot be compared directly with the narrow-band approximation in Fig 7. as the large cycle part is based on the envelope process.

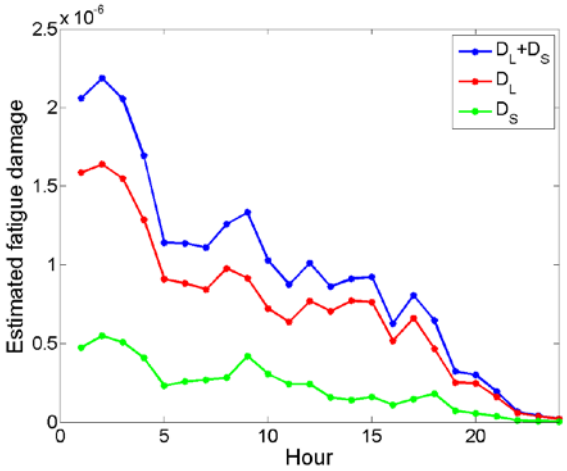

Fig. 9: Fatigue damage during 24 hours on 12 August 2011 estimated using narrow-banded spectral analysis assuming two Gaussian narrow-banded processes.

Combination of two Narrow-banded Gaussian Processes – Correction for Amplification Effects

In the previous method outlined by Jiao & Moan, the small cycle amplitudes were assumed equal to those of the HF process. However, the approach by Low (2010) takes into account two effects which reduce the amplitudes of the small cycles and the large cycles, respectively, and thereby the conservatism of the fatigue damage estimation. It is argued by Low (2010) that the presence of an underlying low frequency process will decrease the amplitude of the small cycles. Furthermore, for the large cycles the cycle amplitude is generally lower than what is obtained by simple addition of the peaks due to the fact that the peak of the HF process cannot always

be assumed to coincide with the peak of the low frequency process. Low (2010) aimed at developing a bimodal method that matches the rainflow counting results more closely than the narrow-band approximations by taking the two mentioned reducing effects into account. According to Low (2010) the small-cycle damage can then be expressed as:

$$D_S = \frac{2^m[\nu_{0,HF} - \nu_{0,WF}]T}{K}\int_0^\infty \int_{\frac{\pi}{4\beta}}^{\frac{\pi}{2}} \int_{\epsilon(r_{WF},\kappa)}^\infty [r_{HF} - \varepsilon(r_{WF},\kappa)]^m \times f_{R_{HF}}(r_{HF}) f_\Theta(\kappa) f_{R_{WF}}(r_{WF}) \mathrm{d}r_{HF}\mathrm{d}\kappa\mathrm{d}r_{WF} \quad (13)$$

where

$$\epsilon(r_{WF},\kappa) = \frac{\pi}{2\beta} r_{WF}\sin\kappa \quad (14)$$

The functions $f_{R_{WF}}(r_{WF})$ and $f_{R_{HF}}(r_{HF})$ are the Rayleigh distributions of the WF and HF processes, respectively. The phase Θ between the peaks of the two processes is assumed uniformly distributed:

$$f_\Theta(\kappa) = \left(\frac{\pi}{2} - \frac{\pi}{4\beta}\right)^{-1}, \qquad \frac{\pi}{4\beta} \le \kappa < \frac{\pi}{2}$$

The triple integration of Eq. (13) must be carried out numerically. However, the innermost integral can be evaluated as a series expansion reducing the problem to two dimensions. The analytical solution to the innermost integral J_S in Eq. (13) reads (Low, 2010):

$$J_S = \int_\epsilon^\infty [r - \varepsilon]^m \frac{r}{s_{HF}^2}\exp\left(-\frac{r^2}{2s_{HF}^2}\right)\mathrm{d}r$$

A binomial series expansion leads to:

$$J_S = \sum_{k=0}^{m}\binom{m}{k}(-\varepsilon)^{m-k} I_k$$

where

$$I_k = \int_\epsilon^\infty r^k \frac{r}{2s_{HF}^2}\exp\left(-\frac{r^2}{2s_{HF}^2}\right)\mathrm{d}r$$

Setting m = 3 the series expansion has four terms and thus the solution for J_S reduces to:

$$J_S = \exp\left(-\frac{\epsilon^2}{2s_{HF}^2}\right)(-3\epsilon s_{HF}^2) + 3(\epsilon^2 + s_{HF}^2)\sqrt{2\pi}s_{HF}\Phi\left(-\frac{\epsilon}{s_{HF}}\right)$$

where $\Phi(\ \ )$ is the standard normal cumulative distribution function (CDF).

Accordingly, the large cycle damage can be expressed as (Low, 2010):

$$D_L = \frac{2^m \nu_{0,WF} T}{\pi K}\int_0^\infty \int_0^\infty \int_0^\pi \{r_{WF}\cos(c(r_{WF},r_{HF})\psi) + r_{HF}\cos[(\beta c(r_{WF},r_{HF}) - 1)\psi]\}^m \times f_{R_{HF}}(r_{HF}) f_{R_{WF}}(r_{WF}) \mathrm{d}\psi\mathrm{d}r_{HF}\mathrm{d}r_{WF} \quad (15)$$

where

$$c(r_{WF},r_{HF}) = \frac{r_{HF}\beta}{r_{WF} + r_{HF}\beta^2}$$

As it was the case for the small cycle damage Eq. (15) is to complex to evaluate analytically. The innermost integral in Eq. (15) reads:

$$J_L = \int_0^\pi \{r_{WF}\cos(c\psi) + r_{HF}\cos([\beta c - 1]\psi)\}^m \mathrm{d}\psi \quad (16)$$

Again, setting m = 3, Eq. (16) can be evaluated analytically allowing Eq. (15) to be solved numerically. The integral can be solved using standard integrations of cosine to power n:

$$\int \cos^3\alpha x\mathrm{d}x = \frac{1}{\alpha}\left(\sin\alpha x - \frac{1}{3}\sin^3\alpha x\right)$$

and

$$\int \cos^2\alpha x\cos\beta x\,\mathrm{d}x = \frac{1}{2\beta}\sin\beta x + \frac{1}{4(2\alpha-\beta)}\sin[(2\alpha-\beta)x] + \frac{1}{4(2\alpha+\beta)}\sin[(2\alpha+\beta)x]$$

The upper limit of the outermost integral in Eq. (13) is set to $5s_{WF}$. In Eq. (15), the upper limit of the outermost integral is also set to $5s_{WF}$ and for the middle integral the limit is set to $5s_{HF}$. Below, the estimated fatigue damage for 12 August 2011 is illustrated in Fig. 10.

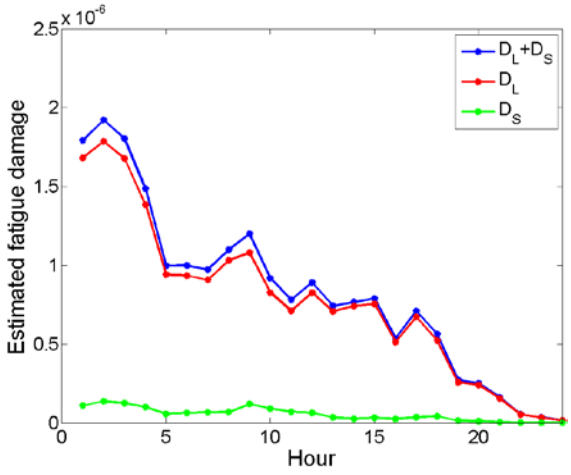

Fig. 10: Fatigue damage during 24 hours on 12 August 2011.

Compared to the previous approach, the method by Low is seen to reduce the contribution of the small cycle damage to the total estimated damage. However, since the small cycles cannot, according to Low, be assumed equal to the HF part of

the process the results from this method cannot be interpreted as the high frequency part of the process having a negligible influence of the total fatigue damage.

Comparison and Discussion of Fatigue Damage Estimation Methods

Generally, a clear correlation between the sea state recorded by WaMoS (Appendix A) and the estimated fatigue damage can be observed even though the estimation of H_S may not be accurate.

In Fig. 11, Fig. 12 and Fig. 13, the results of the fatigue damage estimations are compared for the three days. Only the total damage for the five estimation methods is illustrated. In Fig. 12 the estimate using the method by Low (2012) coincides with the narrow-band approximation (Eq. (1)).

The frequency spacing parameter β, Eq. (7), is illustrated together with the θ-parameter, Eq. (6), illustrating the relative importance of the high frequency process in Fig. 14, Fig. 15 and Fig. 16.

The frequency spacing parameter β is quite constant around 4 with the data for 12 August having the lowest values of β. The narrow-banded approximation is expected to perform better for lower values of β which cannot directly be observed from the analysed sets of data since the variation of β is small here.

It is seen that the data from 12 August are dominated by the HF process, whereas the two other days are dominated by the WF process despite the sea state being more severe on 02 October than on 12 August.

The method by Low, which is aimed at reducing the conservativeness of the spectral analysis, does indeed generally seem to yield results closer to the RFC-results than the three other methods. The exception is 02 October where the estimate using Low's method is the lowest of the five methods, for reasons that are not clear.

In real life, the individual processes in Fig. 3 and Fig. 4 may be well-separated but not necessarily narrow-banded. The total process is clearly not narrow-banded and the individual frequency components cannot generally be considered narrow-banded either. Despite both the total and the individual processes at times clearly being non-narrow-banded the spectral methods generally have good agreement with the outcome of RFC.

Conclusions

In order to assess whether spectral methods for fatigue damage estimation are applicable in onboard systems for monitoring fatigue damage on board ships, four spectral methods for estimating fatigue damage have been applied on full scale measurements of the strains amidships in the hull of a 9400 TEU container ship and compared with the outcome of RFC.

Generally, all four spectral methods assume the total process or at least the individual frequency components of the process to be Gaussian and narrow-banded. However, none of these assumptions are generally true for the analysed measurements. Nevertheless, the agreement between the spectral methods and RFC is generally good and the narrow-band approximation seems to yield a fast and fair estimate of the fatigue damage.

Acknowledgement

The availability of valuable full scale data through the TULCS project is greatly appreciated. Thanks to Eric Wictor and Marcus Schiere for setting up the data files and providing trouble shooting. Sincere thanks to assistant professor Ying Min Low at Nanyang Technological University in Singapore for valuable discussions regarding the application of his method for ocean going ships.

References

Jiao, G, and Moan, T (1990) "Probabilistic Analysis of Fatigue due to Gaussian Load Processes", Probabilistic Engineering Mechanics, Vol. 5, No. 2, pp 76-83.

Low, YM (2010) "A Method for Accurate Estimation of the Fatigue Damage Induced by Bimodal Processes", Probabilistic Engineering Mechanics, Vol. 25, pp 75-85.

Nielsen, UD, Koning, J, and Andersen, IMV (2013) "Comparisons of Means of Estimating the Sea State from an Advancing Large Container Ship", Proceedings of the PRADS2013 (Changwon City, Korea).

Nielsen, UD, Jensen, JJ, Pedersen, PT, and Ito, Y (2011) "Onboard Monitoring of Fatigue Damage Rates in the Hull Girder", Marine Structures, Vol. 24, pp 182-206.

Storhaug, G, Moe, G (2007) "Measurements of Wave Induced Vibrations Onboard a large Container Vessel Operating in Harsh Environment", Proceedings of the PRADS2010 (Houston, Texas), pp 64-72.

MARIN (2007). Installation Report for the Lashing@Sea project.

American Bureau of Shipping (2010) "Guidance Notes on Springing Assessment for Container Carriers"

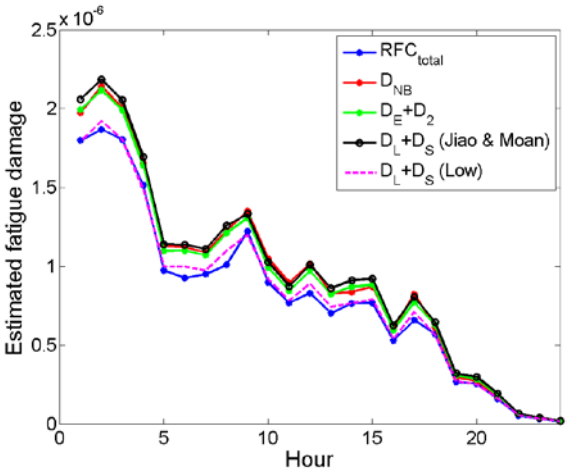

Fig. 11: Comparison of estimated fatigue damage per hour during 24 hours on 12 August 2011. T_0 = 10 sec.

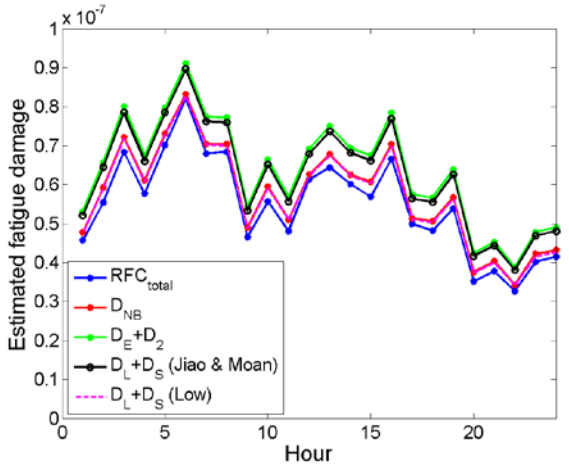

Fig. 12: Comparison of estimated fatigue damage per hour during 24 hours on 20 September 2011. T_0 = 10 sec.

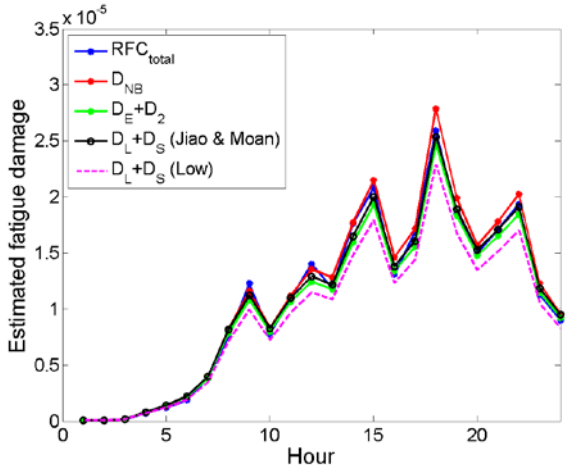

Fig. 13: Comparison of estimated fatigue damage per hour during 24 hours on 02 October 2011. T_0 = 10 sec.

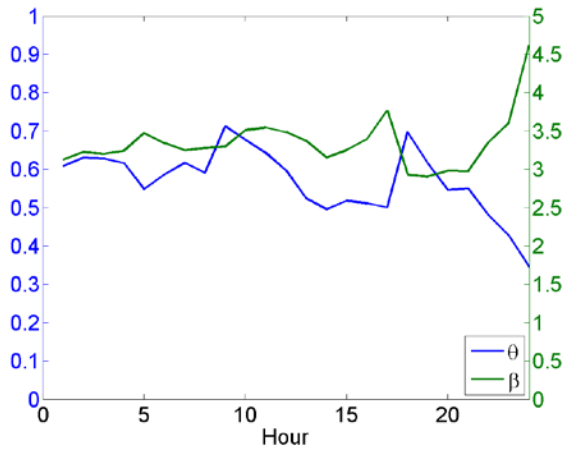

Fig. 14: Relative dominance θ of the HF process and spacing between low and high frequency parts β for 12 August 2011.

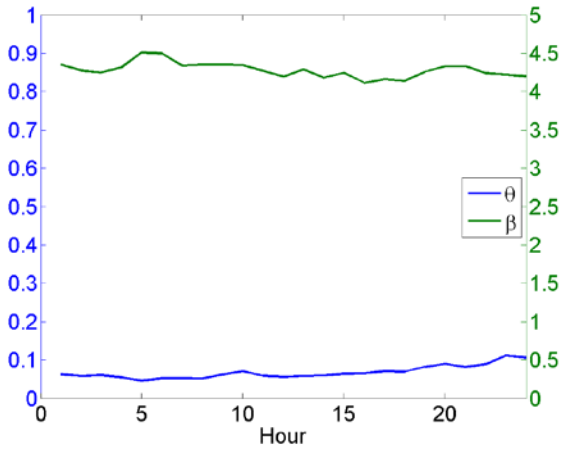

Fig. 15: Relative dominance θ of the HF process and spacing between low and high frequency parts β for 20 September 2011.

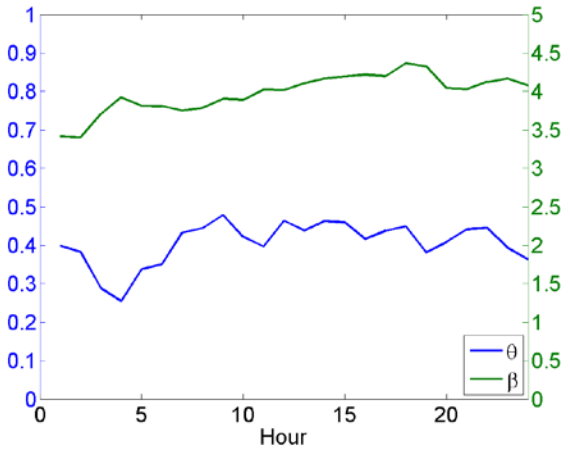

Fig. 16: Relative dominance θ of the HF process and spacing between low and high frequency parts β for 20 September 2011.

Appendix A – Sea State Parameters from WaMoS

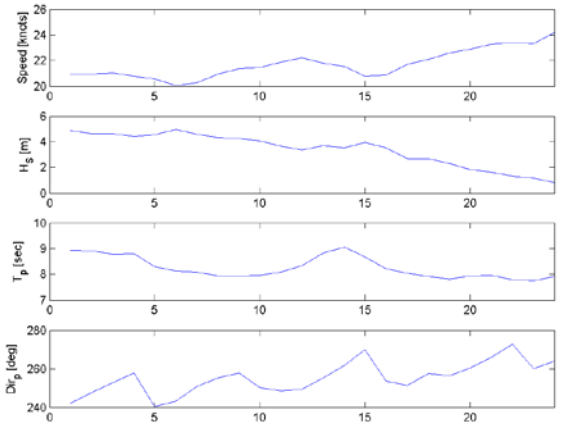

Fig. A1: Navigational and wave data for 12 August 2011 (one hour average, 24 hours of data). Ship speed is speed through water. Peak direction, Dir_p, is given in relation to the ship where 180° is head sea.

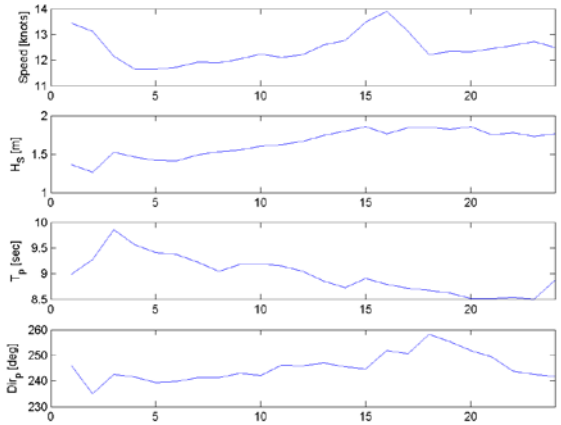

Fig. A2: Navigational and wave data for 20 September 2011 (one hour average, 24 hours of data). Ship speed is speed through water. Peak direction, Dir_p, is given in relation to the ship where 180° is head sea.

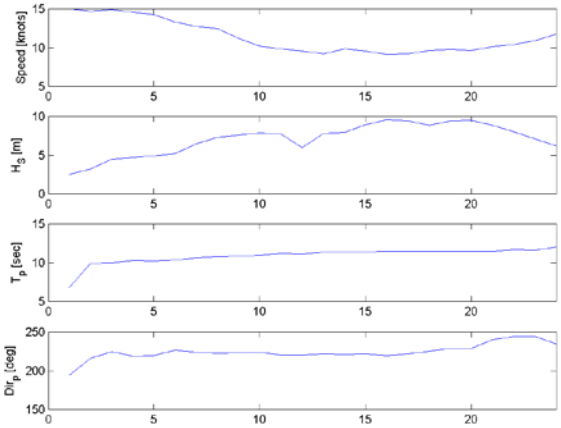

Fig. A3: Navigational and wave data for 02 October 2011 (one hour average, 24 hours of data). Ship speed is speed through water. Peak direction, Dir_p, is given in relation to the ship where 180° is head sea.